NOTATION

I, discharge current; U, voltage applied to the electrodes; E, electric field intensity; ℓ_1 and ℓ_2, distance between the point electrode and the plane of the ring electrode and between the plane of the ring and the cutoff of the tube with the liquid, respectively; P, force of the flow pressure exerted on the target; n_0, number of molecules per unit volume; T, temperature; v, velocity of the phase transformation front; a, coefficient of thermal diffusivity; t, time; $x_m(t)$, coordinate of the melting front relative to the moving evaporation front; r_V and L_V, specific volume heats of evaporation and melting; c_V, specific volume heat capacity; and q, energy flux density.

LITERATURE CITED

1. L. A. Babenya et al., Inzh-Fiz. Zh., 50, No. 6, 951-959 (1986).
2. L. A. Babenya et al., Inzh-Fiz. Zh., 50, No. 5, 729-735 (1986).
3. L. A. Vasil'ev, Schlieren Methods [in Russian], Moscow (1968).
4. S. M. Gorlin and I. I. Slezinger, Aerodynamic Measurements [in Russian], Moscow (1964).
5. V. D. Rusanov and A. A. Fridman, Physics of Chemically Active Plasma [in Russian], Moscow (1984).
6. V. N. Karnyushin and R. I. Soloukhin, Macroscopic and Molecular Processes in Gas Laser [in Russian], Moscow (1981).
7. V. A. Legasov, V. D. Rusanov, and L. A. Fridman, Collection of Articles in Chemistry of Plasma [in Russian], No. 5, B. M. Smirnov (ed.), Moscow (1978), pp. 328-337.
8. A. G. Goloveiko and L. A. Bebenya, "Interaction of atomic particles with a solid," in: Proceedings of the 7th All-Union Conference, Vol. 3, Minsk (1984), pp. 184-187.
9. "Method for vaporization of liquids," Inventor's Certificate No. 1163113 SSSR. F 26 B 3/34.

GENERATORS OF NONEQUILIBRIUM LOW-TEMPERATURE PLASMA

G. Yu. Dautov

UDC 533.9.07

Results are described of a study and of the characteristics of sources of a nonequilibrium gas-discharge plasma.

Plasma chemistry, metallurgy, deposition of coating and films on various details and separators, plasma sharpening and welding, plasma engines, lasers, the handling of surface materials, and MHD-generators are an incomplete list of the promising applications of low-temperature plasma. To enhance the effectiveness of these applications and create new plasma techniques it is necessary to have stability of operational plasma generators, having high efficiency and large resources. For conversion of gas, liquids, and solids into a low-temperature plasma one may use electric discharge energy, laser radiation, electron beams, and chemical fuels. In the present study we consider plasma generators with glow, high-frequency, and arc discharges. The discharges enumerated make it possible to obtain plasma flows in a wide range of variations of sizes, temperatures, and pressures.

The ion mobility in a plasma is substantially smaller than the electron mobility, and therefore the electric field transports its energy mostly by electrons. As a result the kinetic energy of the directed electron motion increases. During collisions the dominant part of this energy is transported by heavy particles (ions, atoms, molecules), consumed by ionization, dissipation of neutral particles, converted into kinetic energy of chaotic thermal electron motion, and the remaining part is transported by the surrounding plasma due to the thermal conductivity. In this connection the electron temperature in a gas discharge

A. N. Tupolev Kazan Aviation Institute.

Translated from Inzhenerno-Fizicheskii Zhurnal, Vol. 53, No. 6, pp. 966-975, December, 1987. Original article submitted July 14, 1986.

0022-0841/87/5306-1434$12.50

plasma is always higher than the heavier component temperature. It hence follows that a low-temperature plasma of electric discharges is, in principle, always a nonequilibrium plasma. Under certain conditions, however, the nonequilibrium may be insignificant and can be neglected. The extent of temperature nonequilibrium can be estimated by using the energy conservation equation of an electron gas. When the discharge is stationary and the electrons lose their excess energy only during elastic collisions, one can obtain the following equation for the temperature difference [1]

$$\frac{T_e - T}{T_e} = \frac{m_a}{4m_e}\left(\frac{\bar{\lambda}_e eE}{\frac{3}{2}kT_e}\right)^2. \quad (1)$$

Account of the electron energy loss during inelastic collisions and due to thermal conductivity, of the nature of gas motion, and of the discharge evolution leads to more complicated quantitative dependences. However, for qualitative description of the separation between T_e and T this equation can be justifiably used. It is seen from Eq. (1) that the relative temperature difference increases with increasing electron mean free path and electric field intensity. In turn, $\bar{\lambda}_e$ increases when the pressure is lowered. For each discharge type E decreases insignificantly with decreasing pressure, and the work of the electric field per mean free path increases. Therefore, the temperature difference increases with reduced pressure, and the role of temperature nonequilibrium in the physical processes becomes significant. Another limiting case

$$\frac{T_e - T}{T_e} \ll 1 \quad (2)$$

is realized in intense arc and high-frequency high-pressure plasmatrons, described in [1-6]. In the present study we consider gas discharge plasma generators in a wide range of parameter variation, when condition (2) is not satisfied. The properties of the generated plasma flow are determined to a large extent by the type of discharge and physical processes occurring in it. Therefore, the theory of electrical gas discharges is the basis of engineering calculations, and is an essential component of describing the characteristics of plasma generators.

1. Plasma Generators with Glow Discharge (PGGD). The first studies of glow discharge (GD) and its applications go back to the mid nineteenth century. A huge number of experimental and theoretical has been accumulated and generalized in a number of monographs [7-9]. Recently the study of GD in gas flows and the creation of promising PGGD have become particularly important in relation to the wide application of GD plasma in quantum electronics, plasma chemistry, industry technology of details of optical devices, and microelectronics. Despite all that, the literature has very few data on PGGD characteristics.

The most widespread PGGD are generators with longitudinal and transverse discharges. Figure 1 shows their main operating schemes. In a PGGD with longitudinal discharge the main part of a long positive column (PC) is located along the flow (Fig. 1a). PGGDs of such a system consist of a cooled cathode 1 and anode 2, and a quartz tube 3. The plasma forming gas in the discharge chamber is fed through tangential or axial apertures, passes through the discharge 5, and emerges from the PGGD in the form of a plasma flow 5. The main advantages of this scheme are the PC stability in space, the possibility of restricting the heating of longitudinal GD, and the high effectiveness of interaction of the flow of plasma forming gas with the discharge. Disadvantages are the low generator power, and a restricted cross section of the plasma flow. Figure 1b shows the schematic diagram of a PGGD with transverse discharge. Its main elements are a cathode 1, a copper anode 2, a plate cathode node 3, and lateral walls 4 of insulating materials. The plasma forming gas is moved in the direction of the arrow. The cathodes are arranged in the form of a rectangular matrix, in which the number of rows is i' and the number of columns is j'. The sequence of cathodes located along the flow is a column, while the sequence located perpendicularly to the flow provides a row. In the case shown in the figure the selection was: i' = 9, j' = 2. It is assumed that the number of rows increasees in the direction of gas flow from 1 to i'. The total number of cathodes equals i'j'. A characteristic feature of this scheme is that the positive columns of discharges 6 are located perpendicularly to the plasma velocity of motion. Selecting i' and j', one can augment the required values of the plasma bulk, the flow sizes 5, and the power, which is a major advantage of PGGD with transverse discharge. Disadvantages are the

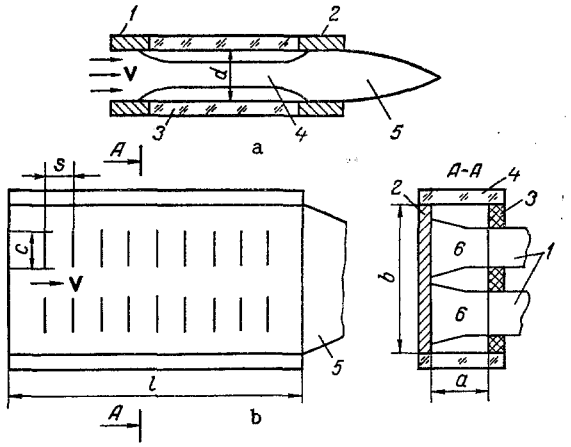

Fig. 1. Schematic diagram of plasma generators with glow discharge.

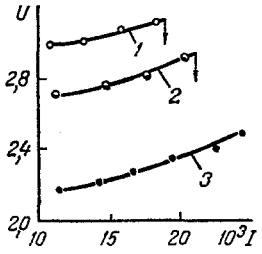

Fig. 2

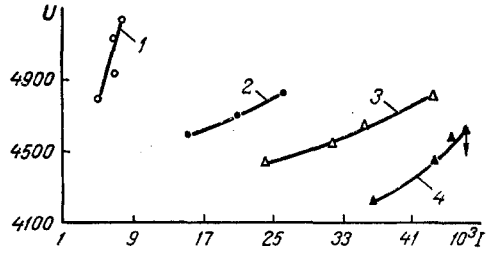

Fig. 3

Fig. 2. The current–voltage characteristics of discharge in longitudinal (curves 1, 2) and vortical (curve 3) air flows: 1) G = 2.65 g·sec^{-1}; 2, 3) 2.2 g·g·sec^{-1}. I, A; U, kV.

Fig. 3. Current–voltage characteristics of transverse discharges in PGGD with s = 40 mm, c = 36 mm, U, V.

complexity of generator construction and of systems of its electric energy power supply, as well as measurement of discharge characteristics through separate cathodes in the direction of plasma flow.

Figure 2 shows the current–voltage characteristics (CVC) of PGGD with longitudinal discharge with d = 2 cm, p = 6600 Pa. As seen from the figure, they are rising. The discharge in a vortical flow is more stable, and its intensity is less than that of discharge in a longitudinal flow. The intensity difference is substantial, and increases with increasing air discharge. The arrows show the CVC points corresponding to the beginning of discharge contraction. The contraction precedes the formation near the anode of a sharply illuminated region with high electric field intensity. Following contraction, E decreases sharply (by 2-4 times), and the gas temperature is significantly enhanced.

Figure 3 shows the CVC of PGGD with transverse discharge for an air–helium mixture with p = $30.2 \cdot 10^3$ Pa, i' = 8, j' = 1, b = 100 mm, a = 30 mm, ℓ = 535 mm, G_B = 8 g·sec^{-1}, G_{He} = 1.6 g·sec^{-1}, where curves 1, 2, 3, 4 correspond to row numbers 1, 2, 7, and 8. The arrows show the critical values of the transition point of GD to an arc. As is seen, the GVC are increasing for all cathodes. By comparing curves 1-4 it follows that for identical current values the discharge intensity decreases below the flow. This is explained by plasma heating and the enhancement of its electric conductivity during the motion process in the generator [10]. The substantial positive differential resistance makes it possible to obtain a stable GD without a ballast resistance, thus enhancing the electric efficiency of the generator. The discharge intensity increases with pressure and mean-mass plasma velocity.

The main features of the generators described of both types are the large cathode potential drop (300-400 V), the high electric field intensity at the PC (200-1200 V·cm^{-1}), a nonequilibrium temperature (for T = 400-600 K the quantity T_e is tens of thousands of degrees),

and substantial population inversion of a number of molecular vibrational levels [7, 11-13]. The characteristics of these PGGD in the stationary regime are described by the equations of motion

$$\rho(\mathbf{V}\,\mathrm{grad})\,\mathbf{V} = \mathrm{div}\,\mathcal{P}, \tag{3}$$

continuity

$$\mathrm{div}\,(\rho\mathbf{V}) = 0, \tag{4}$$

energy conservation for the heavy plasma components

$$\rho(\mathbf{V}\,\mathrm{grad})\,W = \mathrm{div}\,(\mathcal{P}\mathbf{V}) + \mathrm{div}\,(\varkappa\,\mathrm{grad}\,T) + \gamma_1\sigma E^2 + q, \tag{5}$$

equations of state for the plasma comopnents

$$p_i = n_i k T_i, \tag{6}$$

Ohm's law in integral form

$$I = \iint_S \sigma E dS \tag{7}$$

while per unit volume

$$\mathbf{j} = \sigma\mathbf{E}, \tag{8}$$

and continuity equations for the electron and ion gases

$$\mathrm{div}\,[(\mathbf{V} - b_e\mathbf{E})\,n_e - D_e\,\mathrm{grad}\,n_e] = (\alpha_e - \alpha_n)\,n_e + \alpha_0 n_n - \beta n_e n_p, \tag{9}$$

$$\mathrm{div}\,[(\mathbf{V} + b_p\mathbf{E})\,n_p - D_p\,\mathrm{grad}\,n_p] = \alpha_e n_e - \beta n_p n_e, \tag{10}$$

$$\mathrm{div}\,[(\mathbf{V} - b_n\mathbf{E})\,n_n - D_n\,\mathrm{grad}\,n_n] = \alpha_n n_e - \alpha_0 n_n, \tag{11}$$

the Poisson equation

$$\mathrm{div}\,(\varepsilon\varepsilon_0\mathbf{E}) = e(n_p - n_e - n_n), \tag{12}$$

the vibrational kinetic equation

$$(\mathbf{V}\,\mathrm{grad})\,W_{\mathrm{K}} = -\,\mathrm{div}\,\boldsymbol{\Gamma}_{\mathrm{K}} + \gamma_2 jE - q \tag{13}$$

and energy conservation of the electron gas

$$\mathrm{div}\,(\varkappa_e\,\mathrm{grad}\,T_e) + (1 - \gamma_1 - \gamma_2)\,jE = 0. \tag{14}$$

Here γ_1 and γ_2 are the fractions of power jE consumed by heating, gas ionization, and nonequilibrium excitation of molecular vibrational levels, q takes into account the transition of vibrational to thermal energy due to VT relaxation, determined by the equations of vibrational kinetics for the separate molecular shapes with account of VV and VT processes, $\rho = \sum_i n_i m_i$, $p = \sum_i p_i$, and S is the transverse cross section area of camera discharge. To solve this system of equations it is necessary to assign the appropriate boundary conditions, and the quantities α_e, α_n, α_0, β, σ, κ, κ_e, I must be known.

As an example consider the approximate description of physical processes in a PC of longitudinal stationary discharge under PGGD conditions, operating on a CO_2–N_2–He–CO = 1:1:7.9:0.1 mixture. It is assumed that the discharge chamber has a rectangular cross section, the gas flow is directed along the x axis, the plasma properties remain unchanged along the z axis, the cross section y = 0 coincides with the internal chamber surface, and the camera length is substantially larger than its height y_{max}. Analysis of the equations with account of the conditions in the PGGD shows that in the problem under consideration Eqs. (3), (5), and (13) can be written down in the boundary layer approximation, neglecting in (9)-(11) charged particle diffusion along the x axis, neglecting in (5) and (14) heat transport along the x axis due to thermal conductivity, and neglecting in (13) vibrational energy transport along the x axis during the molecular diffusion process [14]. In (7) we took into account the constancy of E over the transverse cross section of the camera discharge. The simplified system of equations was solved by computer. The quantity W_k in (13) was determined from the vibrational kinetic equations for the N_2, CO_2, and CO molecules.

Figure 4 shows the characteristic vibrational temperature distributions of the antisymmetric mode of CO_2 molecules along the discharge chamber for G = 1 g·sec^{-1}, I = 0.3 A,

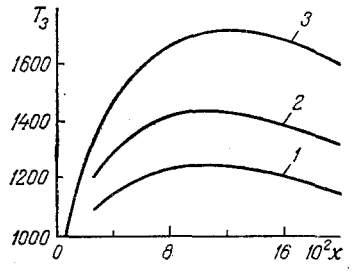

Fig. 4. Vibrational temperature distriution of the antisymmetric mode of CO_2 molecules along the discharge chamber of PGGD with longitudinal flow: 1) y = 0.08 cm; 2) 0.37; 3) 1, x, m; T_3, K.

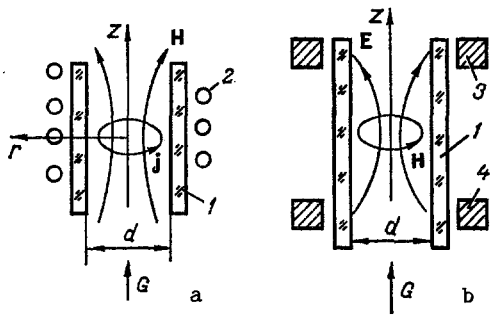

Fig. 5. Schematic diagrams of high-frequency plasmatrons of induction (a) and capacitance (b) types.

$V_x(0, y) = 50$ m·sec^{-1}, $T(0, y) = 300$ K, $0 \leq y \leq 0.02$ m, $0 \leq z \leq 0.1$ m. As is seen from the figure, below the flow T_3 initially increases sharply, reaches a maximum, and then starts decreasing. This nature of T_3 variation is explained by the fact that the VT relaxation time decreases with enhanced gas temperature, and for large lengths of chamber discharge is longer than the gas transition time through the PGGD. Therefore, for large x a substantial part of the vibrational energy transforms to chaotic energy of translational and rotational molecular motions, as a result of which T_3 is reduced. It must be noted that the gas temperature at $y = 10^{-2}$ m increases slowly for the parameters mentioned from 300 K (x = 0) to 470 K (x = 0.2 m). Comparison of these figures with the data of Fig. 4 allow for substantial nonequilibrium of excitation of molecular vibrational degrees of freedom, which is a characteristic feature of PGGD processes, guaranteeing wide application of flow discharge plasma in quantum electronics and plasma chemistry.

Plasma Generators with High-Frequency Discharge (PGHFD) at Low Pressure. Among the PGHFD of various schemes, the most wide spread at the present time are plasmotrons with induction and capacitance discharges. The main schemes are shown in Fig. 5. The main elements of an induction plasmatron are a quartz tube 1 and an inductor 2. A high-frequency current is guided to the inductor from the power supply of the system, creating a variable magnetic field **H** inside the tube with axial component H_z. By the law of electromagnetic induction

$$\mathscr{E}_i = -\frac{\partial \Phi_m}{\partial t} \tag{15}$$

this field creates in the plasma a a variable vortical electric field, generating an annular current j. In a capacitance plasmatron the variable electric field inside the tube 1 is created by means of the electrodes 3 and 4, and the conductivity currents in the plasma are enclosed with electrodes due to current mixing. At high pressures and high discharge powers condition (2) is satisfied, and this case is described in [6] and in other studies. At low pressures the nonequilibrium becomes substantial, and in the discharge region we have almost the same physical processes as in a PC of flow discharge. The main differences consist in that in the plasmatron scheme (Fig. 5a) the electric field is generated due to electromagnetic

induction, regions cathode and anode potential drops are absent, and the electric field intensity is less than in PC of glow discharge. The discharge in the plasmatron scheme (Fig. 5b) differs form the classical GD in that the electrodes 3 and 4 are located behind the limits of the discharge chambers, and the current direction varies with the frequency of the applied voltage.

An important advantage of PGHFD is the high degree of purely obtained plasma (there is no electrode erosion), as well as high opertional resource (thousands of hours). Among the disadvantages one must mention the complexity of the power supply system and the necessity of shielding from the high-frequency electromagnetic field.

The characteristic feture of calculating low-pressure PGHFD consists of the necessity of determining the charged particle concentrations and the electric field intensity from (9)-(12) and the eqution

$$\mathrm{rot}\,\mathbf{H} = \sigma\mathbf{E} + \frac{\partial \varepsilon\varepsilon_0 \mathbf{E}}{\partial t}, \tag{16}$$

$$\mathrm{rot}\,\mathbf{E} = -\frac{\partial \mu\mu_0 \mathbf{H}}{\partial t}, \tag{17}$$

$$\mathrm{div}\,(\mu\mu_0\mathbf{H}) = 0. \tag{18}$$

In this case it is necesary to take into account the variability of the quantities α_e, α_n, α_0, β and the transport coefficients in space. The variation of the plasma state with time can be neglected, since the oscillation period of the high-frequency field in PGHFD is less by many orders of magnitude than the characteristic time of variation of the plasma state. For a plasma in bulk discharge one can put in (16) $\partial\varepsilon\varepsilon_0 E/\partial t = 0$, and in (12) $-(n_p - n_e - n_n) = 0$. However, in the boundary layer region adjacent to the electrodes of the PGHFD scheme (Fig. 5b) the mixing current density $\partial\varepsilon\varepsilon_0 E/\partial t$ can be much higher than the conductivity current density σE. The system of equations (12), (16)-(18) under the assumption of quasineutral plasma, the possibilities of neglecting the mixing current, and with the use of a number of other simplifying assumptions, was solved in [15, 16, and elsewhere]. The results of these papers show that in the PGHFD scheme (Fig. 5a) the magnetic field intensity H_z increases with increasing r, and the electron concentration is reduced. According to the nature of the distributions of the electric field intensity and the electron concentration upon moving away from the axis of the discharge chamber the current density increases, reaching a maximum, and dropping practically to zero near the walls. The electron concentration at the flow axis of an argon plasma at the output of a PGHFD nozzle with p = 1.3...200 Pa, W_p = 0.8...3.0 kW, G = 0.05...0.26 g·sec^{-1} is 10^{10}-10^{12} cm^{-3}. It decreases in the direction of gas flow and with decreasing discharge power [17].

The characteristic feature of low-pressure PGHFD is the existence in them of a bulk discharge, filling practically the whole discharge chamber. With increasing pressure this discharge becomes unstable, and transforms to a contracted form.

3. Plasma Generator with Arc Discharge (PGAD). Generators of this type can be distinguished into plasmatrons with longitudinal and transverse discharges. At the present time the most widespread are plasmatrons with longitudinal discharge. The main scheme of the simplest single-chamber plasmatron coincides with the schematic diagram shown in Fig. 1a. Often, for vortical arc stabilization one uses tangential feed of the plasma forming gas in the discharge chamber. In these cases the plasmatron construction has one or several vortical chambers. A feature of these PGAD is that a substantial part of the PC is located along the plasmatron axis. In [18] were given gas temperature distributions in the discharge chamber for d = 1 cm, p = 10^5 Pa, G = 0.45 g·sec^{-1}, I = 100 A. Analysis of these distributions shows that a plasma with sufficiently high electric conductivity occupies only the small region $0 \leq r < 0.2$ cm. The ratio of the area of this region to the area of the transverse cross section of the discharge chamber $0.25\pi d^2$ is 0.16. Thus, the main part of the gas flows between the PC and the plasmatron wall, and has a low electron concentration. Besides, this part of the gas is found in a strong radial electric field. This field is generated due to the existence of a potential difference between the PC and the walls of the arc chamber. Therefore, a semi-self-maintained discharge is generated here with a high electric field intensity, and the plasma is a nonequilibrium one. It hence follows that a substantial portion of the generated plasma is a nonequilibrium one, and the equilibrium

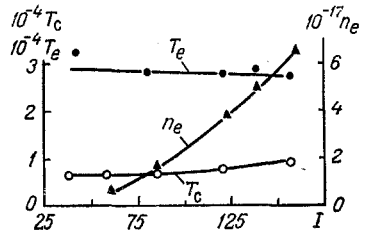

Fig. 6. Mean-mass stagnation temperature of the gas, and the electron temperature and concentration at the flow axis as functions of the arc current; T_c, T_e, K; n_e, m^{-3}.

plasma occupies only a small near-axial region. At low pressures and low currents the plasma equilibrium region vanishes totally, and condition (2) is violated in the whole plasma region inside the PGAD. There exist practically no theoretical studies of arc plasmatrons based on the solution of the system of equations (3)-(14). In the experimental studies the nonequilibrium excitation of vibrational molecular levels, the formation of negative ions, and electron capture have also not been accounted for. Studies of the physical processes occurring in the gas between the PC and the walls of the arc chamber have only started. This is explained by the extreme complication of processes in a nonequilibrium arc plasma, the difficulty of measuring discharge parameters in the boundary-layer region, and the absence of reliable diagnostic methods of nonequilibrium discharge.

To study the flow of an arc plasma, plasmatrons were created, the internal surface of whose discharge chamber had the shape of a hypersonic nozzle. The plasma was treated in a vacuum chamber and was pumped out by a vacuum pump. The arc was passed through the critical cross section in the anode, and its radial portion in the diffusor part had the shape of an umbrella. Air served as a plasma forming gas. In the region of air outlet 0...0.3 $g \cdot sec^{-1}$ the pressure in the vacuum chamber varied from 10^{-1} to 1 Pa. Figure 6 shows the characteristic dependence of the electron temperature and concentration at the flow axis at the outlet from the PGAD nozzle and the mean-mass flow braking temperature T_s on the arc current. As seen from the figure, T_e is $(27-29) \cdot 10^3$ K, while at the same time the T value at the flow axis did not exceed 15,000 K. The strong deviation between T_e and T can be explained by the high electric field intensity on the radial portion of the arc inside the anode and by the low pressure.

Thus, the generators described of nonequilibrium plasmas with various type discharges have been characterized by the physical processes occurring in them. To optimize their construction and characteristics we need further experimental and theoretical studies, the creation of engineering methods of discharge chamber calculations, and the development of effective methods of enhancing the stability of bulk discharges.

NOTATION

x, y, z, Cartesian coordinates; r, φ, z, cylindrical coordinates; t, time; e, absolute value of the electron charge; k, Böltzmann constant; m_e and m, electron and atomic mass; n_e, n_p, and n_n, concentrations of electrons, positive, and negative ions; b_e, b_p, and b_n, mobilities of electrons, positive, and negative ions; D_e, D_p, and D_n, diffusion coefficients of electrons, positive, and negative ions; ε, μ, relative dielectric and magnetic permeabilities; ε_0, μ_0, dielectric and magnetic constants; α_e, α_n, α_0, β, constants of ionization by electron impact, electron capture, loosening, and recombination; T_e and T, temperatures of the electron gas and of the heavy plasma components; ρ, p, κ, σ, density, pressure, thermal conductivity, and electric conductivity; κ_e, thermal conductivity of the electron gas; V, velocity of directional gas flow; W, internal energy; W_k, vibrational energy per unit volume of the gas; Γ_k, flow density of vibrational energy due to diffusion; $\underline{\mathcal{P}}$, viscous stress tensor; j, current density; I and U, discharge current and voltage; λ_e, electron mean free path; G, gas flow rate through the plasma generator; a, b, c, d, ℓ, and s, dimensions of the discharge chamber; Φ_m, flux vector of magnetic induction; $\mathcal{E}_i$, emf of electromagnetic induction; W_p, discharge power; and T_c, mean-mass stagnation temperature of the gas.

LITERATURE CITED

1. V. Finkel'nburg and G. Mecker, Electric Arcs and Thermal Plasma [Russian translation], Moscow (1961).
2. A. G. Shashkov, Heat Exchange in Electric Arc Gas Heaters [in Russian], Moscow (1974).
3. M. F. Zhukov, A. S. Koroteev, and B. A. Uryukov, Applied Dynamics of a Thermal Plasma [in Russian], Novosibirsk (1974).
4. O. I. Yas'ko, Electric Arc in a Plasmatron [in Russian], Minsk (1977).
5. G. Yu. Dautov, V. L. Dzyuba, and I. N. Karp, Plasmatrons with Stabilized Electric Arcs [in Russian], Kiev (1984).
6. S. V. Dresvin (ed.), Physics and Technology of Low-Temperature Plasma [in Russian], Moscow (1972).
7. Yu. P. Raizer, Foundations of Contemporary Physics of Gas-Discharge Processes [in Russian], Moscow (1980).
8. V. L. Granovskii, ELectric Currents Established in Gases [in Russian], Moscow (1973).
9. A. Zigel', Ionized Gases [in Russian], Moscow (1959).
10. G. Yu. Dautov, F. M. Gaisin, Z. M. Bedretdinov, and A. N. Nikitin, Low-Temperature Plasma [in Russian], Kazan' (1979).
11. B. F. Gordiets, A. I. Osipov, and L. A. Shelepin, Kinetic Processes in Gases and Molecular Lasers [in Russian], Moscow (1980).
12. V. N. Karnyushin and R. I. Soloukhin, Macroscopic and Molecular Processes in Gas Lasers [in Russian], Moscow (1981).
13. E. P. Velikhov, V. S. Golubev, and S. V. Pashkin, Usp. Fiz. Nauk, 137, No. 1, 117-150 (1982).
14. I. G. Galeev and B. A. Timerkaev, Physics of Flowing Gas-Discharge Systems [in Russian], Minsk (1986), pp. 111-119.
15. H. U. Eckert, J. Appl. Phys., 33, No. 9, 2780-2788 (1962).
16. I. Sh. Abdullin and F. A. Sal'yanov, Izv. Sib. Otd. Akad. Nauk SSSR, Ser. Tekh. Nauk, No. 13, 100-103 (1981).
17. I. G. Gafarov, G. I. Ibragimov, A. M. Minnigulov, and V. A. Osadchii, Low-Temperature Plasma [in Russian], Kazan (1984), pp. 17-22.
18. N. G. Dautova, N. G. Zalyalov, R. S. Tukhvatullin, and R. M. Khairullin, Zh. Prikl. Spektrosk., 22, No. 6, 978-980 (1975).